



DOI: doi.org/10.21009/SPEKTRA.082.01

THE COMPARISON OF 2D DOSE PATIENT-SPECIFIC QUALITY ASSURANCE BETWEEN MONTE CARLO-CONVOLUTION AND MODIFIED CLARKSON INTEGRATION ALGORITHM

Akbar Azzi*, Supriyanto Ardjo Pawiro, Terry Mart

Department of Physics, Faculty of Mathematics and Natural Sciences, Universitas Indonesia, Indonesia

*Corresponding Author Email: akbar.azzi@sci.ui.ac.id

Received: 4 March 2023
Revised: 5 June 2023
Accepted: 9 July 2023
Online: 21 August 2023
Published: 30 August 2023

SPEKTRA: Jurnal Fisika dan Aplikasinya
p-ISSN: 2541-3384
e-ISSN: 2541-3392



ABSTRACT

A sophisticated machine of radiotherapy treatment process follows the complexity of the quality assurance (QA) measurement. Non-measurement QA becomes one of the solutions to reduce the medical physicists' workload. However, this method has not been clinically established. This study compared two non-measurement methods of patient-specific quality assurance (PSQA) to find the feasible algorithm for the adaptive radiotherapy process. Monte Carlo-based (MC) PSQA used a phase space file of the medical linear accelerator (Linac) to obtain the photon energy fluence and forward projected to the isoplane. In contrast, Modified Clarkson Integration-based (MCI) used a non-uniform fluence map in the isoplane. For the modulated intensity, we used a pair of the dynamic log files of the multileaf-collimator (MLC) and then employed them in the algorithms. The dose distributions of MC and MCI methods were compared to the treatment planning system (TPS) using gamma index analysis. We found that the gamma pass rates (GPR) for MC-TPS and MCI-TPS were 99.54% and 99.57%, respectively. Further, the dose distribution in the off-axis region for the MCI method showed lesser accuracy due to the higher secondary dose contribution. The linac log file information can be used and calculated into a 2D dose distribution using both MC and MCI methods, providing high-accuracy results.

Keywords: patient-specific quality assurance, log files, 2D dose calculation algorithm

INTRODUCTION

The radiation oncology process of treating cancer is divided into image acquisition, dose plan, and dose delivery. Among these parts, there is a connecting software called oncology information systems (OIS), such as Mosaiq and Aria. Image acquisition is performed by using dedicated computer tomography (CT) scan, then saved in digital imaging and communications in medicine (DICOM) format. This digital image is transferred to the treatment planning system (TPS), with which oncologists and medical physicists plan the radiation dose. An approved plan, which has plan parameters such as isocenter position, monitor units, gantry angle, jaws position, and multi-leaf collimator (MLC) position, is exported to the linear accelerator (Linac) console through the OIS [1]. Furthermore, the Linac delivers the radiation based on the plan parameter. Linac also records the beam status and mechanical movement during the irradiation and stores it in the log. This log's low frequency is also sent back to the IOS and saved in the database [2].

Verification between planned and delivered doses is one of the workloads of medical physicists in the clinical routine. The purpose of verification is to ensure whether the dose plan in TPS agrees with the treated dose. The common dose verification is measurement-based, which uses a set of detectors such as an electronic portal image device (EPID) or 2D ionization array before the first irradiation is given to the patient [3]. However, a novel non-measurement-based dose verification is adopted in the verification. One of the examples is using the log file information as the input for a secondary dose check [4]. Several studies have developed quality assurance based on log files in different ways, such as recalculation of the log file to the TPS algorithm [5] or log file as an input for secondary dose/MU calculation for Varian [6] and Elekta Linac [7]. In the Elekta, the machine log is stored every eight previous days with a 25 Hz frequency for each file. However, the patient information is not given inside the log. In contrast, the Varian log has two times lower frequency than Elekta. However, in the latter the patient information is stored inside the file.

Dose verification as a PSQA based on log files is powerful for adaptive radiotherapy due to the process's less time-consuming time than the measurement-based PSQA. Adaptive radiotherapy is a technique that evaluates the outcome of the treatment during the whole radiotherapy process. The evaluation mainly observed the change in the patient body structure that impacts tumor target volume or organs at risk (OAR) [8]. Adaptive radiotherapy has been shown to have merit in decreasing the toxicity effect of normal tissue because of the tumor's sinking in the second or third week after the first beam treatment [9]. Log file-based verification could evaluate the treatment in each fractionation. As a result, the accuracy of treatment would be improved. Combined with onboard imaging such as cone beam computed tomography (CBCT), preventive action could be performed if the patient's structure is changed or the error in the machine is shown. An independent dose calculation also impacts on reducing the error of PSQA. Several methods of independent dose calculation are currently used in clinics, such as factor-based, model-based, and Monte Carlo [10, 11]. In this research, we compared the Monte Carlo-Convolution (MCC) and Modified Clarkson Integration (MCI) algorithms for 2D dose verification to understand the resistances of the log file as an input of the secondary dose calculation algorithm.

METHOD

Monte Carlo – Convolution

The Monte Carlo Convolution method combines Monte Carlo simulation on head Linac and fluence-energy dose kernel convolution inside the phantom body as seen in FIGURE 1, respectively. In Varian Linac, the head simulation was using BEAMnrc user code. The output of this simulation was called *phase space file* that consists of the fluence particle, energy, direction, and angular momentum. In this work, we separated the fluence and energy using *beamdp* user code. On the other hand, we used International Atomic Energy Agency (IAEA) *phase space file* for Elekta Linac [12, 13]. Both *phase space file* was generated below the collimator mirror structure of head Linac. The fluence was projected to the isoplane and the information of the log file was inserted to the fluence. We created the *energy deposit kernel* (EDK) with *edknrc* user code of Monte Carlo from spherical water density and 8 variation energies from 1 to 6 MeV of photon to distribute the projected fluence in the phantom geometry. The convolution method used the EDK and projected photon fluence to obtain dose distribution, which follows.

$$D(r) = \iint \varphi(r') \left(\frac{\mu}{\rho} \right) \otimes EDK(r, r') d^2 r' \quad (1)$$

where r and r' are the observed points relative to the centers of EDK and fluence, respectively. $D(r)$ is the dose at point r , and $\varphi(r')$ is the photon fluence at point r' . For the detailed parameters of this Monte Carlo simulation, we refer the readers to the previous reports [14, 15].

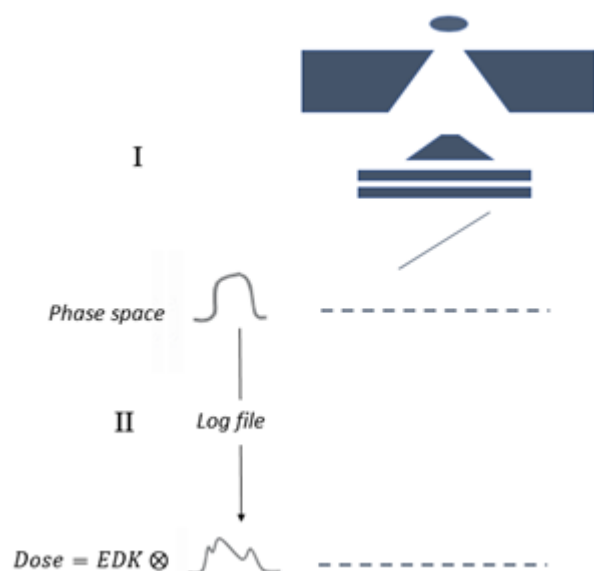


FIGURE 1. Monte Carlo-Convolution dose scheme. Phase I is the Monte Carlo simulation and *phase space file* output. Phase II is the convolution of projected fluence and *energy deposit kernel* (EDK).

Modified Clarkson Integration

Clarkson’s method in principle is a factor-based calculation to achieve a dose point from irregular field size radiation. The main concept of this method is isolating the primary and secondary photon fluences. The primary photon fluence is independent of field size and collimator which block the trace of ray [16]. Furthermore, Clarkson’s method is modified for two-dimensional dose calculation to enable the intensity modulated radiotherapy (IMRT) factor. Modified Clarkson method utilizes polar coordinate because of the secondary photon fluence was distributed in 360 degrees direction. In general the MCI calculation follows.

$$D(x, y) = MU(r) \left[D_p(x, y) + \sum D_s(x, y) \right] \tag{2}$$

where $D(x,y)$, $D_p(x,y)$, and $D_s(x,y)$ are the total, primary, and secondary doses at x dan y positions in the Cartesian coordinate. $MU(r)$ is derived from $MU(x,y)$ in polar coordinate with radius of r . The MCI calculation in this work refers to the previous work [11].

Linear Accelerator Log Files

Linac log file consists of irradiation mechanism information and is written after the treatment has been done. This information is stored, but not directly accessible. In Varian, the log could be retrieved after each fraction. However, additional console 4DITC must be activated before the treatment. In Elekta, the log file could be extracted in service mode. The machine would collect all the treatment information in the past eight days. The example of the Varian and Elekta log file is shown in FIGURE 2.

In this study, we have selected four information within the log file i.e. control points, dose per fraction, jaws position, and MLC position. The gantry angle position was set to 0 degree for all calculation. These parameter was transformed to two-dimensional shape in isoplane position by using MATLAB. It was necessary to project the log parameter to isoplane because of the actual MLC position was 30-45 cm from x-ray target but the photon fluence was at 100 cm from the target. The MLC also had a round tip end which effected to the projected position because of beam penumbra. We used EQUATION (3) to solve this error based on American Association of Physicists in Medicine (AAPM) Report No 50 [18-20].

Current dose fraction	Segment number	Beam state	Segment dose index	Gantry rotation	Collimator rotation	Upper Y1 jaw position	Lower Y2 jaw position	Upper X1 jaw position	Lower X2 jaw position	Leaf actual position (first)	Leaf actual position (...)	Leaf actual position (last)
4.68	1	Radiation	9	179.9	0	49.9	52.5	0.1	-0.5	14.2	...	12.8
4.72	1	Radiation	9.3	179.9	0	49.9	52.7	0.1	-0.6	14.2	...	12.8
...

Time	Control point	Linac State	Actual Dose Rate	Step Dose	Wedge Position	Step Gantry	Step Collimator	Table Position	X1 Diaphragm	X2 Diaphragm	Y2 Leaf (first)	Y2 Leaf (...)	Y2 Leaf (last)	Y1 Leaf (first)	Y1 Leaf (...)	Y1 Leaf (last)
358	1	0	410	615	1	1800	1800	2796	50	58	-3468	...	-2856	3350	...	3580
433	1	0	410	820	1	1800	1800	2796	50	58	-3468	...	-2856	3350	...	3580
...

FIGURE 2. Typical log file information of Varian (top) and Elekta (bottom). Control points, dose per control point, jaws position, and MLC position were extracted from log file in this work.

$$x = \frac{W \cdot SCD \pm R \cdot SAD \left(1 - \frac{SAD}{\sqrt{SAD^2 + W^2}} \right)}{SCD \pm R \frac{W}{\sqrt{SAD^2 + W^2}}} \quad (3)$$

where x is the MLC position at range of interest from target (W). SAD (*source to axis distance*) and SCD (*source to collimator distance*) are the ranges from target to the isoplane and target to the MLC, respectively, while R is the radius of round shape at the end-tip of MLC.

Evaluation methods

The 2D dose distributions of MCI and MCC were compared and evaluated by using the gamma index analysis [20]. EQUATION (4) showed the gamma passing evaluation.

$$\gamma = \sqrt{\left(\frac{\Delta D}{DD} \right)^2 + \left(\frac{\Delta d}{DTA} \right)^2}$$

$pass \rightarrow \gamma \leq 1$ (4)

where ΔD is the percentage dose difference between MCI and MCC. Δd is the distance between point evaluation MCI and MCC in millimeters. This study's DD (dose difference) and DTA (distance to agreement) criteria are 3% dan 3 mm. The pass would be declared if the gamma was equal to or less than 1.

RESULT AND DISCUSSION

Modified Clarkson Integration and Monte Carlo Convolution are two different methods used to calculate dose distributions in radiotherapy. MCI is a deterministic method that uses a series of analytical equations to calculate the dose. In contrast, MCC is a Monte Carlo coupled with a Convolution method that uses a computer to randomly generate photons and track their paths through the patient's body.

The 2D dose evaluation was done on 7 fractionated IMRT patient for Varian Linac and 1 database for volumetric arc radiotherapy (VMAT) technique in Elekta. The dose distribution was normalized to global maximum of dose in each calculation. The example of 2D dose distribution for both machine and algorithm were displayed in FIGURE 3.

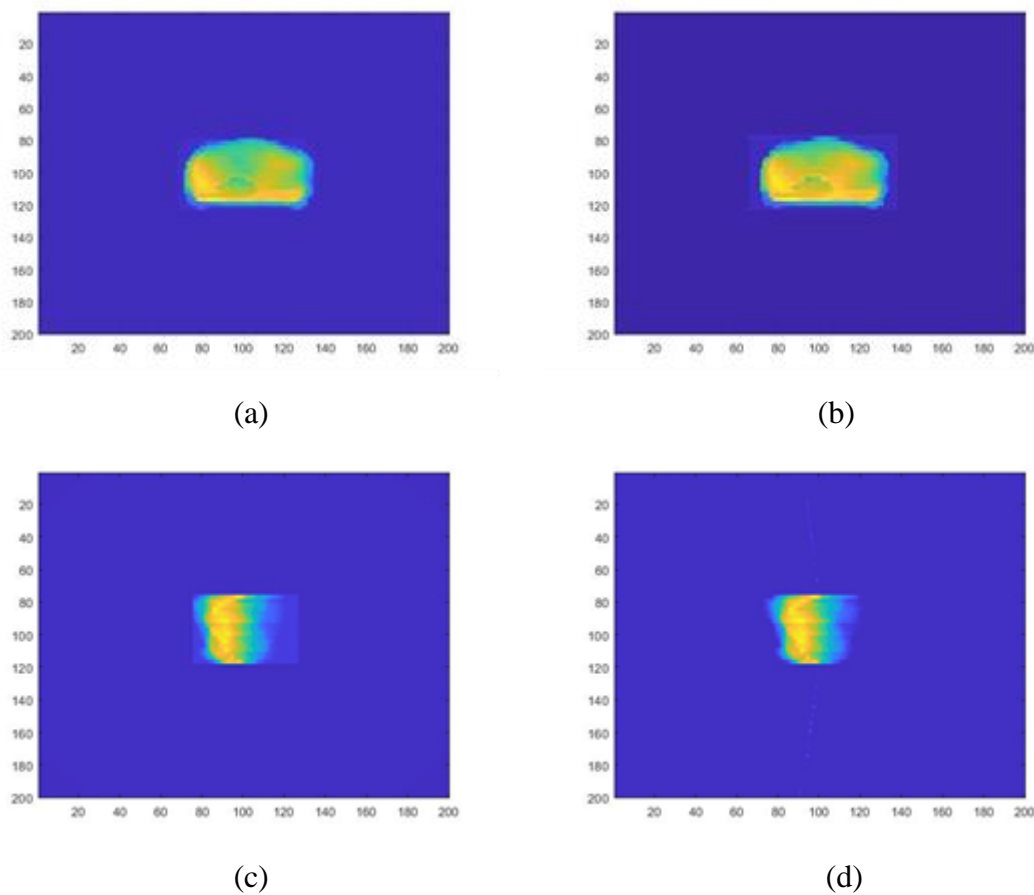


FIGURE 3. 2D dose distribution of Varian Linac with MCC (a) and MCI method (b); and Elekta Linac with MCC (c); and MCI method (d).

In FIGURE 3 (a) and (b) the dose difference between MCC and MCI is visually compared. The dose distribution from MCC is relatively lower than MCI in the central of isoplane. A beam hardening of the flattening filter in Monte Carlo simulation process of head Linac component is the main issue in this finding. As seen in FIGURE 1, the photon from the x-ray target will directly interact with the cone shape of the flattening filter. The lower energy of the photon would be penetrated the middle of the flattening filter. As a result, the photon spectrum after this interaction is shifted to the right or higher energy. This result corroborates the finding of Tsiamas et.al, which showed that photon energy below 1 MeV was less dominant in the interaction because of the beam hardening effect and the scatter will tend to be forward scattered after the collision with matter [21]. On the other hand, 2D dose distribution on MCI method had extra dose at the periphery boundaries because the MCI method was sensitive to secondary photon fluence. The results was agreed with Mubarok et al that the MCI method gain higher error to the TPS at the radiation field edge [11]. The main principles of Clarkson's method was the calculation of the dose point in the center of the field axis [22]. The off-axis of this method could be developed for higher accuracy. In addition, several studies found that MCI is less accurate than Monte Carlo simulation for complex dose distributions and is recommended for one point secondary dose check or simple geometry dose verification [23, 24].

Both MCC and MCI method had a good agreement with TPS based on the gamma index analysis. All the Varian 2D dose calculations had 95% pass rate of gamma with 3%/3mm criteria as seen in TABLE 1.

TABEL 1. Percentage of gamma passing rate (GPR) of 2D dose calculation of Varian Linac for Monte Carlo-convolution and Modified Clarkson Integration to Treatment Planning System.

No	GPR MCC-TPS (%)	GPR MCI-TPS (%)
1	99.02	99.40
2	98.95	99.57
3	99.64	99.61
4	100.00	99.80
5	99.92	99.56
6	99.90	99.33
7	99.34	99.71
Mean	99.54	99.57
Deviation	0.41	0.15

The comparative results of MCC and MCI method for Elekta Linac were evaluated by using gamma index analysis. The MCI method is set as a reference in this evaluation. FIGURE 4 shows the distribution of gamma and its histogram. The dot line outside the radiation field size as mentioned of the extra dose at FIGURE 3(b) and (d) expressed as the fail condition in this gamma analysis. A better view of this results as seen in FIGURE 4(a) and the gamma was around 1.5. The global gamma index pass rate within 200×200 piksel area had 98.85%.

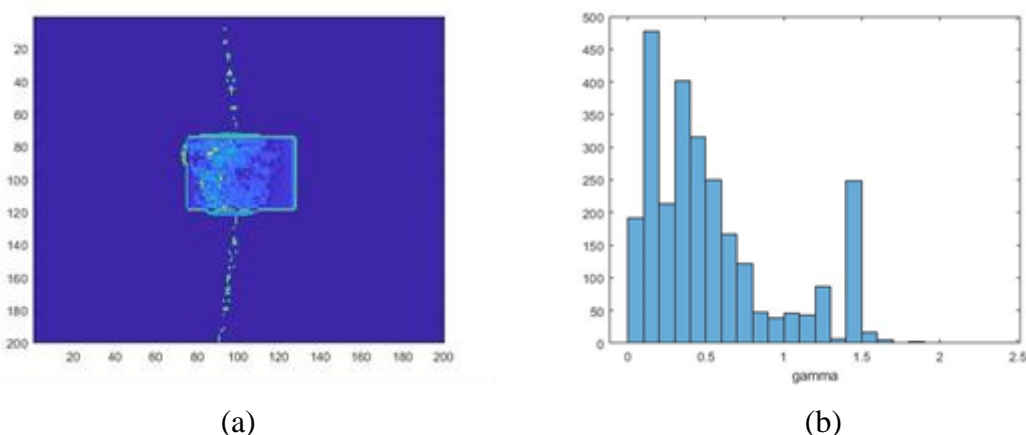


FIGURE 4. 2D gamma distribution (a) and histogram (b) of MCC and MCI algorithm for Elekta Linac.

CONCLUSION

Using the log file for the dose calculation based on MCC and MCI algorithms for patient-specific quality assurance yielded good results with a gamma index pass rate was more than 95%. In each algorithm, the gamma index was 98.85% for 3%/3mm criteria. However, the off-axis in MCI calculation has an extra dose because of the MLC movement between control points. Besides, the MCC algorithm had a beam hardening issue on the central axis of photon fluence. There is still room for developing PSQA with log files based on the Monte Carlo-Convolution and Modified Clarkson Integration method.

ACKNOWLEDGEMENT

The authors thank Sayid Mubarak for the fruitful discussion on the MCI algorithm code. The elekta log file was downloaded online from Simon Biggs <https://doi.org/10.5281/zenodo.2594333>. This research is supported by the PUTI grant from the University of Indonesia under contract number NKB-664/UN2.RST/HKP.05.00/2022.

REFERENCES

- [1] A. Yazdanian, "Oncology Information System: A Qualitative Study to Identify Cancer Patient Care Workflows," *Journal Of Medicine and Life*, vol. 13, no. 4, pp. 469-474, 2020, doi: 10.25122/jml-2019-0169.
- [2] S. Kirmann *et al.*, "Visualization of data in radiotherapy using web services for optimization of workflow," *Radiation Oncology*, vol. 10, no. 1, pp. 1-12, 2015, doi: 10.1186/s13014-014-0322-3.
- [3] A. Chendi *et al.*, "EPID-based 3D dosimetry for pre-treatment FFF VMAT stereotactic body radiotherapy plan verification using dosimetry CheckTM," *Physica Medica*, vol. 81, pp. 227-236, 2021, doi: 10.1016/j.ejmp.2020.12.014.
- [4] P. D. H. Wall *et al.*, "Prospective Clinical Validation of Virtual Patient-Specific Quality Assurance of Volumetric Modulated Arc Therapy Radiation Therapy Plans," *International Journal of Radiation Oncology, Biology, Physics*, vol. 113, no. 5, pp. 1091-1102, 2022, doi: 10.1016/j.ijrobp.2022.04.040.
- [5] J. W. Lee *et al.*, "Inverse verification of the dose distribution for intensity modulated radiation therapy patient-specific quality assurance using dynamic MLC log files," *Journal Korean Physics Social*, vol. 55, no. 4, pp. 1649-1656, 2009, doi: 10.3938/jkps.55.1649.
- [6] C. Han *et al.*, "Cross verification of independent dose recalculation, log files based, and phantom measurement-based pretreatment quality assurance for volumetric modulated arc therapy," *Journal Applied Clinical Medical Physics*, vol. 21, no. 11, pp. 98-104, 2020, doi: 10.1002/acm2.13036.
- [7] Y. Katsuta *et al.*, "Patient-Specific Quality Assurance Using Monte Carlo Dose Calculation and Elekta Log Files for Prostate Volumetric-Modulated Arc Therapy," *Technology in Cancer Research & Treatment*, vol. 16, no. 6, pp. 1220-1225, 2017, doi: 10.1177/1533034617745250.
- [8] W. Lu *et al.*, "Adaptive fractionation therapy: I. Basic concept and strategy," *Physics in Medicine & Biology*, vol. 53, no. 19, pp. 5495-5511, 2008, doi: 10.1088/0031-9155/53/19/015.
- [9] L. Belshaw *et al.*, "Adaptive radiotherapy for head and neck cancer reduces the requirement for rescans during treatment due to spinal cord dose," *Radiation Oncology*, vol. 14, pp. 1-7, 2019, doi: 10.1186/s13014-019-1400-3.
- [10] W. Z. Chen *et al.*, "Impact of dose calculation algorithm on radiation therapy," *World Journal of Radiology*, vol. 6, no. 11, p. 874, 2014, doi: 10.4329/wjr.v6.i11.874.
- [11] S. Mubarak, W. E. Wahyu and P. A. Supriyanto, "2D dose reconstruction of IMRT patient-specific QA based on log file," *Radiation Physics and Chemistry*, vol. 166, p. 108473, 2020, doi: 10.1016/j.radphyschem.2019.108473.

- [12] M. R. McEwen, I. Kawrakow and C. K. Ross, "The effective point of measurement of ionization chambers and the build-up anomaly in MV x-ray beams," *Medical Physics*, vol. 35, no. 3, pp. 950-958, 2008, doi: 10.1118/1.2839329.
- [13] E. Tonkopi *et al.*, "Influence of ion chamber response on in-air profile measurements in megavoltage photon beams," *Medical Physics*, vol. 32, no. 9, pp. 2918-2927, 2005, doi: 10.1118/1.2011090.
- [14] S. A. Pawiro, A. Azzi and D. S. Soejoko, "A Monte Carlo Study of Photon Beam Characteristics on Various Linear Accelerator Filters," *Journal of Biomedical Physics & Engineering*, vol. 10, no. 5, p. 613, 2020.
- [15] A. Azzi, S. A. Pawiro and T. Mart, "3D dose reconstruction of 6 MV medical linear accelerator based on modified ray tracing algorithm: A preliminary result," *AIP Conference Proceedings*, vol. 2346, no. 1, pp. 1-8, 2021, doi: 10.1063/5.0047744.
- [16] M. Pourkaveh *et al.*, "Optimization of Clarkson's method for calculating absorbed dose under compensator filters used in intensity-modulated radiation therapy," *Journal of Biomedical Physics & Engineering*, vol. 10, no. 5, pp. 575-582, 2020, doi: 10.31661/jbpe.v0i0.858.
- [17] C. Böhm and M. Hofer, "Basic Applications of Multileaf Collimators," *AAPM Report Task Group*, 2001.
- [18] W. Yao and J. B. Farr, "Determining the optimal dosimetric leaf gap setting for rounded leaf-end multileaf collimator systems by simple test fields," *Journal of Applied Clinical Medical Physics*, vol. 16, no. 4, pp. 65-77, 2015, doi: 10.1120/jacmp.v16i4.5321.
- [19] M. S. Huq *et al.*, "A dosimetric comparison of various multileaf collimators," *Physics in Medicine & Biology*, vol. 47, no. 12, 2002, doi: 10.1088/0031-9155/47/12/401.
- [20] D. A. Low *et al.*, "A technique for the quantitative evaluation of dose distributions," *Medical Physics*, vol. 25, no. 5, pp. 656-661, 1998.
- [21] P. Tsiamas *et al.*, "Beam quality and dose perturbation of 6MV flattening-filter-free linac," *Physica Medica*, vol. 30, no. 1, pp. 47-56, 2014, doi: 10.1016/j.ejmp.2013.02.004.
- [22] P. R. M. Storchi, L. J. Van Battum and E. Woudstra, "Calculation of a pencil beam kernel from measured photon beam data," *Physics in Medicine Biology*, vol. 44, no. 12, pp. 2917-2928, 1999, doi: 10.1088/0031-9155/44/12/305.
- [23] T. C. Zhu *et al.*, "Report of AAPM Task Group 219 on independent calculation-based dose/MU verification for IMRT," *Medical Physics*, vol. 48, no. 10, pp. e808-e829, 2021, doi: 10.1002/mp.15069.
- [24] H. A. Alkhatib *et al.*, "Output calculation of electron therapy at extended SSD using an improved LBR method," *Medical Physics*, vol. 42, no. 2, pp. 735-740, 2015, doi: 10.1118/1.4905375.

